RSC Advances

Plasma-assisted multi-layered coating towards improved gas permeation properties for organosilica membranes

Journal:	*RSC Advances*
Manuscript ID:	RA-ART-05-2015-008052.R2
Article Type:	Paper
Date Submitted by the Author:	30-Jun-2015
Complete List of Authors:	Ren, Xiuxiu; Hiroshima University, Department of Chemical Engineering Kanezashi, Masakoto; Hiroshima University, Department of Chemical Engineering Nagasawa, Hiroki; Hiroshima University, Department of Chemical Engineering Tsuru, Toshinori; Hiroshima University, Department of Chemical Engineering

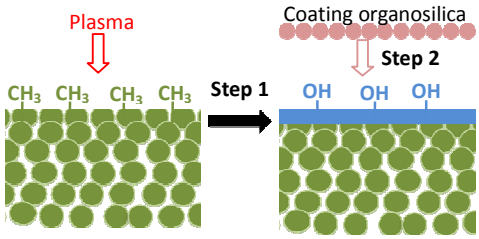

Plasma treatment enhanced separation performance of multi-layered membranes consisting of hydrophobic top-layer and hydrophobic intermediate-layer.

RSC Advances

ARTICLE

Plasma-assisted multi-layered coating towards improved gas permeation properties for organosilica membranes

Xiuxiu Ren, Masakoto Kanezashi, Hiroki Nagasawa, and Toshinori Tsuru*

Hydrophobic silica membranes for gas separation are proposed to achieve high gas permeation properties in the presence of water vapor. Hydrophobic Me-SiO_2 sols were prepared by using tetraethoxysilane (TEOS) and methyltrimethoxysilane (MTMS) as co-precursors, coated on macroporous α-Al_2O_3 supports through multi-layered coatings to form an intermediate layer with pore size of approximately 2 nm. H_2O vapor plasma was used for the modification of hydrophobic Me-SiO_2 intermediate layer by generating hydrophilic groups on the surface without changing either the bulk hydrophobicity or the pore size. After plasma treatment of the Me-SiO_2 layers, bis(triethoxysilyl)ethane (BTESE)- or bis(triethoxysilyl)octane (BTESO)-derived sols were coated as separation layers. The gas selectivity for BTESE membrane was improved after water plasma treatment, which allowed better adhesion between each layer via the enhanced hydrophilic modification by water plasma. Under wet conditions, the CO_2 permeance for both membranes were decreased, slightly larger decrease than for membranes without plasma treatment, but much less than the BTESE and BTESO membranes prepared on hydrophilic SiO_2-ZrO_2 intermediate layers. High gas permeation properties were obtained in the presence of water for organosilica membranes prepared from hydrophobic top layers to hydrophobic intermediate layers via plasma-assisted multi-layered coatings.

Received 00th January 20xx,
Accepted 00th January 20xx

DOI: 10.1039/x0xx00000x

www.rsc.org/

Introduction

Porous ceramic membranes with superior thermal and chemical stability have been widely applied in gas separation, pervaporation, membrane reactors and desalination.[1-5] High performance can be attained based on their tunable pore sizes and adsorption ability. The surface chemistry of ceramic membranes is generally hydrophilic, which allows them to enhance water permeability in liquid separation and promote gas permeation in gas separation.[3-5] However, gas permeation typically decreases when these membranes are used under wet atmosphere such as in the practice of removing CO_2 from flue gases or natural gas.[6-9] This is because the hydrophilicity of ceramic membranes results in water capillary condensation in the pores and/or adsorption on the pore walls, which reduce the effective pores and prohibits gas transport. Therefore, ceramic membranes with hydrophobic properties are required for various applications under wet conditions.[10]

Porous silica membranes are commonly fabricated with three layers: α-alumina support layer (pore size: 100-50 nm), intermediate layer (5-1 nm), and ultrathin silica top-layer (0.1-0.6 nm). The top layer mainly determines the permeability and selectivity. The thin top layer can provide a high flux of gas because the transport rate of a gas is in inverse proportion to the thickness of the membrane. The intermediate layers are coated on the support in order to prevent the penetration of silica sols into the support and form the ultrathin top layers. Until now, almost all hydrophobic silica membranes reported consisted of hydrophobic top layers prepared on hydrophilic intermediate layers such as γ-Al_2O_3, SiO_2-ZrO_2 or TiO_2,[11-15] as schematically shown in Fig. 1 (a). Although the intermediate layers make no contribution to the separation performance, water capillary condensation in the pores and/or adsorption on the pore walls could occur, which may reduce gas permeance in the hydrophilic intermediate layers. According to calculations using the Kelvin equation, these hydrophilic layers will allow capillary condensation of water at a relative humidity of 14-68% for diameters ranging from 1-5 nm at room temperature. de Vos et al.[14] prepared hydrophobic membranes by coating hydrophobic MeSi (400) top layers on hydrophilic γ-Al_2O_3 intermediate layers. It was found some stabilization time was still needed for drying the hydrophobic membrane prior to conducting the gas permeance experiment. They concluded water adsorbed in the supported MeSi(400) membranes that was likely to be present in the hydrophilic γ-Al_2O_3 intermediate layers only using Kelvin relation. In our previous works, the hydrophobic membranes such as bis(triethoxysilyl)ethane (BTESE, Si-$(CH_2)_2$-Si) or bis(triethoxysilyl)octane (BTESO, Si-$(CH_2)_8$-Si)-derived sols were also formed on hydrophilic SiO_2-ZrO_2 intermediate layers, and the gas permeation properties were evaluated in the presence of water vapor.[15] We found that the CO_2 permeance was

Department of Chemical Engineering, Hiroshima University, 1-4-1 Kagamiyama, Higashi-Hiroshima,739-8527, Japan. E-mail: tsuru@hiroshima-u.ac.jp; Tel: 082-424-7714; Fax: 082-424-5494

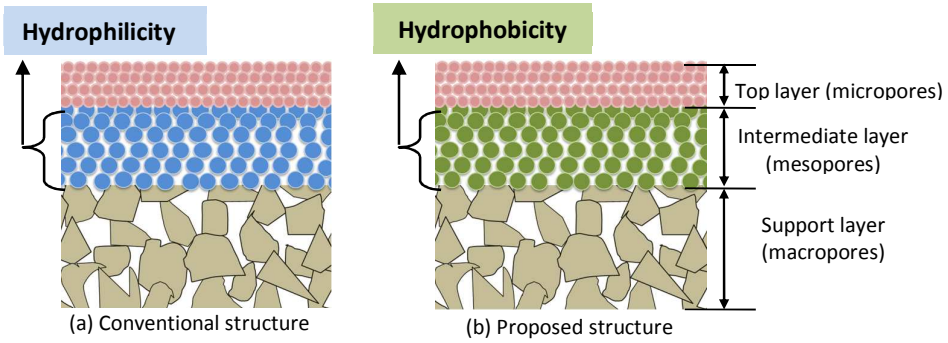

Fig. 1 Schematic structures of the porous organosilica membranes supported on intermediate layers.

drastically decreased in the presence of water vapor. Thus, the introduction of hydrophobicity to an intermediate layer is necessary in real applications to avoid capillary condensation of water in humid process streams, as shown in Fig. 1 (b).

Silica membranes are fabricated according to well-known polymeric sol-gel routes. Alkoxides are hydrolyzed and condensed under acid or base catalysts to form sols in sizes less than 100 nm. Pore size and surface chemistry can be tuned through different precursors. To reduce defects during the formation of thin films, multi-layered coatings are commonly used via sol-gel method. Prosser et al.[16] reported that silica films fabricated by multiple spin-coating would increase in thickness in a linear fashion as a function of the number of coatings, which reduced the tendency of the films toward cracking compared with a single-layer coating. Depagne et al.[17] reported thin silica film (<500 nm) that was built up using a multi-layered approach. However, as far as the authors know, no paper has yet reported the use of multi-layered coatings in the formation of hydrophobic membranes.

Highly permeable and selective organosilica membranes were prepared on hydrophilic intermediate layers.[18-21] The condensation reactions of hydrophilic groups between coated sols and substrates were expected to enhance membrane performance. To fabricate high-performance hydrophobic membranes, the hydrophobic surface which can be ascribed to a small number of -OH groups, should be modified to be more hydrophilic. The plasma technique has been used to activate a hydrophobic surface into a hydrophilic one in a very thin layer without changing the bulk properties.[22-24] Zarshenas et al.[25] reported that the corona air plasma treatment induced polar groups on the surface of membranes, which led to improved gas separation properties without damaging the separation layers. Therefore, to further improve the performance of hydrophobic organosilica membranes, the use of plasma-assisted modification should be investigated, particularly for multi-layered coating.

In the present work, hydrophobic Me-SiO_2 sols were first prepared by co-hydrolysis and polymerization of TEOS and methyltrimethoxysilane (MTMS), and were coated on macroporous α-alumina supports to fabricate Me-SiO_2 nanoporous intermediate layers. The plasma method was then used to modify the hydrophobic surface of the Me-SiO_2, thereby converting to hydrophilic surface chemistry. Finally, BTESE or BTESO-derived sols were coated on the plasma-treated surface to form separation layers. The effect of plasma on multi-layered coating was studied and the gas permeation properties of the hydrophobic organosilica membranes were examined under both dry and wet conditions.

2. Experimental

2.1 Preparation of silica sols

Hydrophobic Me-SiO_2 sols, which were used for the formation of intermediate layer, were prepared using TEOS and MTMS as co-precursors. Two alkoxides (molar ratio TEOS/MTMS=1) dissolved in C_2H_5OH were added with H_2O and ammonia as a catalyst in a bottle in a single step, according to a method established in a previous report.[26] The colloidal size of Me-SiO_2 sols based on the alkaline-catalyst was 10-50 nm, which was suitable for fabrication of mesoporous intermediate layers.[27]

Two types of organosilica sols were prepared for the top layer, using bridged alkoxide bis(triethoxysilyl)ethane (BTESE) and bis(triethoxysilyl)octane (BTESO) via the hydrolysis-condensation process. The precursor was dissolved in ethanol, and then added with water and the acid catalyst HCl under continuous stirring at 25 °C to develop stable and clear silica sols. The chemical structures of BTESE and BTESO consisted of 2 and 8 -CH_2 chains in the linking units between the 2 Si atoms, as shown in Fig. 2.

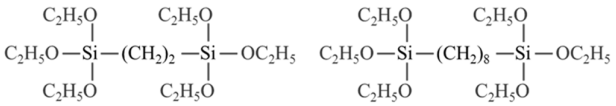

(a) BTESE (b) BTESO

Fig. 2 Structures of bridged organoalkoxysilanes used in this work (a) Bis(triethoxysily)ethane (BTESE) and (b) Bis(triethoxysily)octane (BTESO).

2.2 Preparation of silica films and membranes

Prior to silica coatings, the silicon wafers as substrates were heated at 550 °C for 1 hour in an oxidation furnace for pre-treatment. Hydrophobic films, including $MeSiO_2$, BTESE and BTESO, were all prepared via the spin-coating method. In the spin-coating process, the spin speed was increased up to 5000 rpm in 5 s and was held for 25 s.

Me-SiO_2 sols (1 wt%) were spin-coated twice on these silicon wafers at room temperature, followed by calcination at 400 °C under N_2 atmosphere for 30 min. One coating-cycle involved 2 rounds of spin-coating and 1 round of calcination. This coating cycle was repeated up to 4 times. Then the surface was wiped with a cloth to investigate the adhesion of the multi-coated layers. In a similar manner, BTESE or BTESO sols (1 wt%) were spin-coated twice on silicon wafers or Me-SiO_2 films, followed by drying and calcinating at 300 °C under N_2 atmosphere for 30 min. As before, 1 cycle involved 2 rounds of spin-coating followed by 1 round of calcination. The cycle was repeated up to 4 times and then wiping treatment was performed with a cloth on the surface of the films.

Asymmetric organosilica membranes were fabricated using porous α-alumina tubes. The average pore size of the support was 1-2 μm with an outside diameter of 10 mm. Two types of α-Al_2O_3 suspensions (1 wt%) were prepared by using α-Al_2O_3 particles (2 and 0.2 μm) mixed with 2 wt% silica-zirconia (SiO_2-ZrO_2) solutions as a binder. First, the α-Al_2O_3 suspensions with the size of 2 μm were slip-coated with a cloth on the outer surface of the support and then were fired at 550 °C. The step was repeated three times to cover the larger pores on the support. Second, 0.2 μm α-Al_2O_3 suspensions were further coated and then fired at 550 °C. The coating was repeated five times to form a pore size of less than 100 nm. Third, Me-SiO_2 sols (1 wt%, 10-50 nm colloidal sols) were then coated onto the pre-heated support (200 °C), followed by firing at 400 °C in N_2. The pore size of the intermediate layer was controlled to within approximately 2 nm by coating for several times. Finally, BTESE or BTESO sols that were several nanometers in size were coated on the intermediate layer to form a top layer, followed by drying and calcination at 300 °C for 30 min in N_2. The schematic diagram of membrane fabrication was shown in Fig. S1 (Supporting information).

2.3 Plasma treatment on silica films and membranes

Plasma-assisted modification was conducted on the surface of films and membranes. Films or membranes were first placed into a plasma chamber (BPD-1H, SAMCO, Inc.), and were evacuated to 2 Pa via a vacuum pump. H_2O with the addition of N_2 was used at a power of 10 W for 20 s at room temperature. The flow rates of H_2O vapor and N_2 were controlled at 15 ml/min and 10 ml/min, respectively, and the pressure was maintained at 20 Pa.

2.4 Characterization of hybrid organosilica films

The hybrid organosilica films formed on silicon wafers via spin-coating were characterized at room temperature by Fourier transform infrared (FT-IR) spectroscopy (FT-IR-4100, JASCO). The hydrophilicity of the silica films was evaluated using a microscopic contact angle meter with FAMAS software (DropMaster DM-300, KYOWA INTERFACE SCIENCE, Co., Ltd). The asymmetric structures of membranes were characterized by cross-section of Field Emission Scanning Electron Microscopy (FE-SEM, S-4800, HITACHI) images.

2.5 Gas Permeation Measurement

Gas permeance was evaluated under dry and wet conditions. A schematic diagram of the apparatus for dry gas permeation can be found in a previous paper.[20] Prior to measurement, the membrane was dried first by helium at 200 °C. The pressure difference across the membranes was maintained at 1 bar, and the permeate stream was maintained at atmospheric pressure. Dry gas permeance data in this study was average value of 3 samples with a deviation that was less than 10%. For the permeation of gas/water vapor mixtures, CO_2 gas was bubbled through water and mixed with dry CO_2 gas in the feed stream at atmospheric pressure. Water activities were controlled via the flow rate of the dry and wet streams and measured using a hygrometer (HygroFlex, error range: ±2%RH, Rotonic, Switzerland). In the permeate stream, N_2 was used as sweep gas to carry permeated CO_2 and water vapor continuously to CO_2 sensor (GMT221 and GMT222, error range: ±0.02% and 20 ppm, Vaisala, Finland) and the hygrometer. The equipment was maintained at a temperature of 40 °C. The values for CO_2 and H_2O permeance were calculated using the following equations:

$$P_i = \frac{F_i}{A} \bullet \frac{1}{\Delta p_i} \qquad (1)$$

F_i is the permeated molar flow rate of the component *i*, Δp_i is the logarithmic average partial pressure of component *i* for permeation, and *A* is the effective membrane area. The measurement was repeated five times for experimental data, and the error range was found to be less than 5% for CO_2 and 15% for H_2O permeance.

The gas selectivity, α, was calculated by the following equation as the permeance ratio of each gas:

$$\alpha_{i/j} = \frac{P_i}{P_j} \qquad (2)$$

P_i and P_j represent the permeance of *i* and *j*, respectively.

3. Results and discussion

3.1 Multi-coated thin films on silicon wafers

The FT-IR spectra of Me-SiO_2 films via multiple spin-coating on the silicon wafers are shown in Fig. 3 (a). The contact angles (CA) and peak area are summarized as a function of coating times, as shown in Fig. 3 (b). The peak area of intensity was calculated by integrating the absorbance from 1300-979 cm^{-1} to reveal the quantity of coated films. [28] Since silicon wafer was used as the background in the FT-IR spectra measurement, the peak area was 0 and the CA of silicon wafer was 30° at the

coating time of 0. In Fig. 3 (a), the peak intensity at around 1100 cm^{-1} and 1280 cm^{-1} can be ascribed to Si-O-Si and -CH_3, respectively, and these were obviously increased with increases in the coating times. The contact angles were increased from 30° to 120° after 1 time coating and remained constant even after additional coating times increased, which indicated that the surface of Me-SiO_2 films was highly hydrophobic and the substrate was fully covered by Me-SiO_2 layers. The peak area in the range of 979-1300 cm^{-1} increased in a linear trend for up to 4 times coating. The linear increase in the peak area indicates that the thickness of each coating was approximately the same, confirming excellent multi-layered coatings on hydrophobic surfaces. El-Feky et al. reported preparing hydrophobic silica (Hyd-Si) from TEOS and MTES, silanol groups were mostly replaced by hydrophobic groups of –CH_3. The films showed a contact angle of 108° after firing at 400 °C. The hydroxyl groups remained in the structures of $Q^3[Si(OSi)_3(OH)]$, $Q^2[Si(OSi)_2(OH)_2]$ and $T^2[RSi(OSi)_2(OH)]$ according to the characterization of powdered samples by solid-state ^{29}Si MAS NMR.[29] The -OH groups allowed a uniform film by multi-layered coatings through the condensation of silanol groups.

Fig. 4 (a) (b) and (c) (d) show the characterization of BTESE and BTESO films on silicon wafers, respectively. The peaks at around 1000-1100cm^{-1} that can be ascribed to Si-O-Si groups increased as the coating times increased for both BTESE and BTESO films. The peak areas ranging from 959-1180cm^{-1} for both films were approximately linear increase with coating times. The CA values for two films reached a constant above one-time coating. BTESE films showed a CA of 62°, which was a hydrophilic surface by comparison with BTESO films, which showed a CA of 82°.

The characterization of Me-SiO_2, BTESE and BTESO films coated on silicon wafers showed different properties. The CA was on the order of Me-SiO_2>> BTESO >BTESE. Based on the increase in the peak area per time coating, the thickness of Me-SiO_2 was the largest of the three silica films, probably due to the larger size of the sols and higher viscosity. After the wiping treatment, the peak area was decreased for Me-SiO_2 (Fig. 3 (b)) and BTESO (Fig. 4 (d)), which illustrated a low degree of adhesion between layers. However, the BTESE film showed no change in the absorbance area after wiping treatment, which indicated the strong adhesion between each

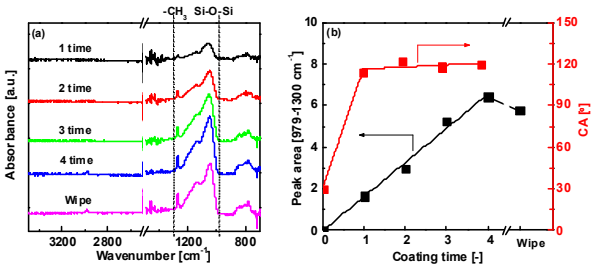

Fig. 3 Characterization of Me-SiO_2 films coated on silicon wafers by (a) FT-IR (b) contact angles and peak areas.

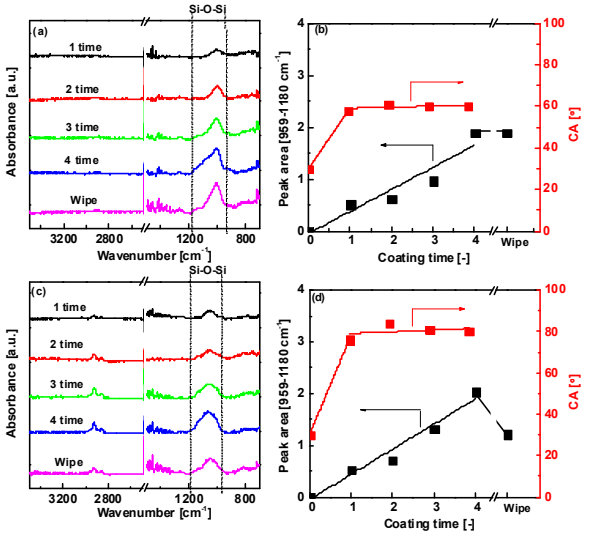

Fig. 4 Characterization of BTESE films on silicon wafers by (a) FT-IR, (b) contact angles and peak area; and BTESO films on silicon wafers by (c) FT-IR, (d) contact angles and peak area.

layer due to the greater number of -OH groups on the surface, as confirmed by the value of CA. The large degree of condensation from the silanol groups between the surface of the sub-layer and the coated sols enhanced the adhesion of the films.

3.2 Multi-coated thin films on Me-SiO_2 layers and the effect of plasma treatment

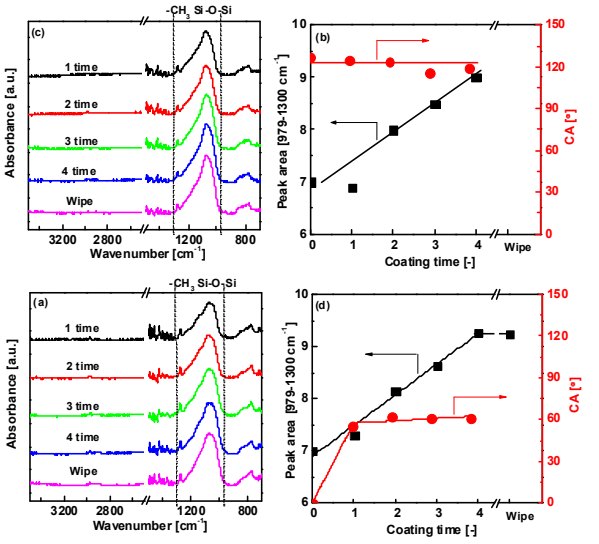

Fig. 5 FT-TR and CA of BTESE coated on Me-SiO_2 films without (a)(b) and with (c)(d) plasma treatment as a function of coating times.

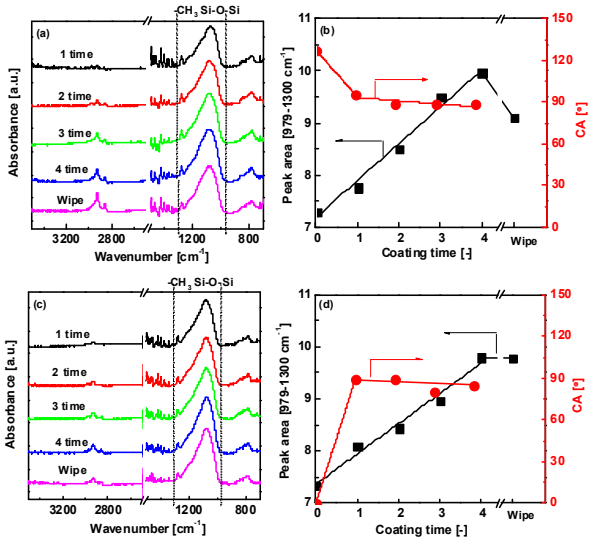

Fig. 6 FT-TR and CA of BTESO coated on Me-SiO_2 films without (a)(b) and with (c)(d) plasma treatment as a function of coating times.

To prepare a hydrophobic top layer on hydrophobic substrates, BTESE sols were spin-coated on Me-SiO_2 layers which had been pre-coated 4 times of Me-SiO_2 on silicon wafers. After coating, BTESE sols were visibly scattered on the surface of Me-SiO_2 layers, and formed separated domains on the Me-SiO_2 films. The FT-IR spectra, CA and peak area are shown in Fig. 5 (a) and (b). The CA remained at nearly 120°, which was the value of Me-SiO_2 layers, and confirmed that BTESE sols could not form homogenous and continuous films on a hydrophobic Me-SiO_2 layer. Considering that BTESE sols were well coated on the hydrophilic silicon wafer (Fig. 4), plasma treatments were applied to introduce hydrophilic groups on the hydrophobic surface of Me-SiO_2 layer to improve the coating properties of BTESE films. The surfaces of films were treated with H_2O-N_2 plasma at 10W at room temperature. During the plasma process, H_2O was excited to hydroxyl radical, atomic and molecular fragments, which reacted with the chemical groups on the surface of Me-SiO_2. After plasma treatment of Me-SiO_2 films for 20 s, the contact angles of the surface became 0°. Then BTESE sols were immediately coated on the plasma-treated films. Fig. 5 (c) and (d) show the characterizations of BTESE films after plasma treatment. The contact angles were decreased as coating times of BTESE increased, and became constant at approximately 60°, which was almost equivalent to that of BTESE films coated on silicon wafers (Fig. 4 (b)). This indicates that BTESE-derived sols fully covered on the surface of Me-SiO_2, formed homogenous and continuous films. The plasma treatment was suitable for BTESE coating on hydrophobic Me-SiO_2 films.

The BTESO films coated on Me-SiO_2 layers are characterized in Fig. 6 (a) and (b). The peak intensity was obviously increased as the coating times increased. The contact angles were decreased and became constant at 88° as coating times increased, which was approximately the same value as BTESO films coated on silicon wafers (Fig. 4 (d)). The peak area was also increased linearly with the coating time, indicating BTESO could form films with a uniform thickness. BTESO and BTESE formed films with different morphology when coated on Me-SiO_2 layers, which may have been due to the differing chemical structures. BTESO sols consisted of hydrophobic portion from the 8 -CH_2 chains in the linking units between the two Si atoms. The hydrophobic portion of BTESO could attach to the hydrophobic Me-SiO_2 surface, while the BTESE sol was repelled due to a higher concentration of silanol groups.

Plasma treatment was also performed on the Me-SiO_2 layer to further coat the BTESO films, as shown in Fig. 6 (c) and (d). The FT-IR spectra and CA were the same for BTESO films coating on Me-SiO_2 surface with and without plasma treatment. However, the peak area showed quite a different tendency in wiping treatment. The peak area was largely decreased after the wiping of BTESO films without plasma treatment (Fig. 6(b)), which was similar to BTESO coating on silicon wafers (Fig. 4 (d)). However, the absorbance area was not decreased for BTESO films with plasma treatment, suggesting that the adhesion force between each layer had been enhanced. This was because the species of hydroxyl radicals, the atomic and molecular fragments in H_2O-plasma process had activated the surface of Me-SiO_2, which changed the surface to reactive sites such as -OH groups.[29] The reactive sites on the Me-SiO_2 surface reacted with the silanol groups (Si-OH) of BTESO sols, and fixed BTESO on the surface.[30] Thus, it is suggested that water plasma is a better method for the multi-coating of hydrophobic sols on hydrophobic films.

3.3 Plasma treatment for multi-coated membranes

3.3.1 Characterization of Me-SiO_2 layers by plasma treatment

To prepare high-performance, thin-layered hydrophobic membranes, we proposed the use of plasma to treat the surface of hydrophobic Me-SiO_2 layers. Steen M. et al.[32] used H_2O plasma treatment on asymmetric polysulfone at a power of 25 W for 2 min that rendered membranes permanently hydrophilic and completely wettable. To avoid a thick-layer modification of hydrophobic Me-SiO_2 layers, the power and time were kept as low as 10 W and 20 s, respectively.

Me-SiO_2 intermediate layers were evaluated by

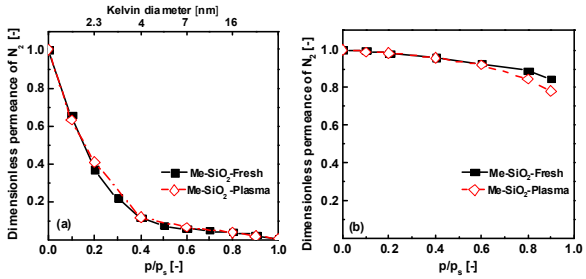

Fig. 7 Nanopermporometry characterization of Me-SiO_2 layers with plasma treatment using (a) hexane and (b) water as condensable vapors.

nanopermporometry before and after H_2O plasma treatment, as shown in Fig. 7. Nanopermporometry is based on the capillary condensation of vapor and the blocking effect of the permeation of non-condensable gases such as N_2.[27,33] The dimensionless permeance of N_2 (DPN), normalized with N_2 permeance under dry conditions, is plotted as a function of the relative pressure of hexane (Fig. 7(a)) and water vapor (Fig. 7 (b)). Kelvin diameter was calculated under an assumption of complete wetting of hexane in pores, and is shown in the top x-axis for reference.

The DPN decreased with an increase in the relative pressure of hexane (Fig. 7(a)), while it was not decreased in the water vapor (Fig. 7(b)). This was because hexane could capillary-condense in $MeSiO_2$-derived pores, whereas water vapor could not, indicating that the pores of Me-SiO_2 layers were hydrophobic. As shown in Fig. 7(a), the pore size distribution evaluated by hexane vapor was unchanged after plasma treatment, while the hydrophobicity of the bulk membranes obtained from water vapor (Fig. 7(b)) was only slightly decreased after plasma treatment. The water plasma was confirmed to convert only the surface properties of Me-SiO_2 from hydrophobicity to hydrophilicity without damaging either the bulk hydrophobicity or the pore size.

3.3.2 Gas permeation properties of organosilica membranes under dry conditions

After plasma treatment, separation layers using BTESE and BTESO sols were deposited on Me-SiO_2 layers. The performance of these membranes for gas separation under dry conditions is shown in Fig. 8. The comparisons with membranes coated on Me-SiO_2 (without plasma) and SiO_2-ZrO_2 layers are summarized in Table 1. BTESE/Me-SiO_2-P membrane (BTESE sols coated on plasma-treated Me-SiO_2 layers) showed high permeance for He and H_2, which was similar to membranes BTESE/Me-SiO_2 without plasma. As the kinetic diameters of gas increased, the differences in gas permeance for the two membranes became significant. The selectivity of H_2/N_2 was 15 and 7 for BTESE/Me-SiO_2-P and BTESE/Me-SiO_2 membranes, respectively. Moreover, the selectivity of H_2/SF_6 was 3005 for BTESE/Me-SiO_2-P membrane,

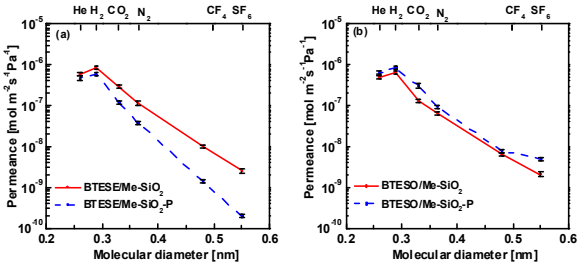

Fig. 8 Single gas permeance at 200 °C for (a) BTESE and (b) BTESO membranes coated on Me-SiO_2 with and without plasma treatment.

which was approximately 10 times higher than for BTESE/Me-SiO_2 membrane. This indicated that defects from uncovered intermediate layers were present in BTESE/Me-SiO_2 membrane. This is confirmed by the surface of the SEM images in Fig. S2 (see Supporting information). The BTESE/Me-SiO_2 membrane showed several uncoated pinholes and a rough surface. The separation properties of gases are extensively dependent on the surface layer (separation layer). When the coatings of surface layer causes any defects, the membranes will not demonstrate good performance. BTESE/Me-SiO_2-P membrane had a smooth and homogeneous surface layer and showed high performance in gas separation. On the other hand, the selectivity of H_2/SF_6 for BTESE/Me-SiO_2-P membrane was close to that of BTESE membrane coated on the hydrophilic SiO_2-ZrO_2 intermediate layers. This may have been due to the hydrophilic properties for both plasma-assisted Me-SiO_2 layers and SiO_2-ZrO_2 layers, since both layers showed contact angles of 0°. The hydrophilic surface of intermediate layers can make BTESE coatings form homogeneous and continuous surface layer without defects.

For BTESO membranes, the gas permeance and selectivity was nearly the same with and without plasma treatment (Fig. 8 (b)). The selectivity for BTESO membranes coated on Me-SiO_2 and Me-SiO_2-P layers was also approximately the same as when BTESO was coated on SiO_2-ZrO_2 intermediate layers. This was probably due to the hydrophilic-hydrophobic portions of

Table 1. Comparison of gas selectivity of organosilica membranes top layer: BTESE, BTESO) prepared on three types of intermediate layers (Me-SiO_2-P (plasma treatment), Me-SiO_2 and SiO_2-ZrO_2) at 200 °C.

Selectivity	BTESE (top layer)			BTESO (top layer)		
	Me-SiO_2-P	Me-SiO_2	SiO_2-ZrO_2[15]	Me-SiO_2-P	Me-SiO_2	SiO_2-ZrO_2[15]
H_2/N_2	15	7	24	9	10	8
H_2/CO_2	5	3	4	3	5	2
CO_2/CF_4	84	29	-	40	20	73
H_2/SF_6	3,005	334	>10,000	170	316	446

BTESO sols. When substrates showed hydrophilic properties (SiO_2-ZrO_2 and plasma treated Me-SiO_2), the end of hydrophilic -OH groups of BTESO attached to the substrates. On the contrary, the hydrophobic long -CH_2 chains will attach to the hydrophobic Me-SiO_2 surface. The permeance and selectivity were not changed but the adhesion was improved after plasma treatment according to the characterizations of the peak area in Fig. 6 (d).

BTESE membranes showed a higher selectivity of H_2/SF_6 than BTESO membranes with either Me-SiO_2-P or SiO_2-ZrO_2 intermediate layers. This was due to the structure differences between BTESE and BTESO. BTESE with 2 methylene groups between two Si atoms formed microporous structures that were suitable for gas separation, while BTESO with 8 methylene groups, which are more flexible, showed dense structures.[15]

3.3.3 Gas permeation of organosilica membranes with plasma treatment in the presence of water vapor

BTESE/Me-SiO_2-P and BTESO/Me-SiO_2-P membranes, both of which were treated with plasma, were examined in the presence of water vapor for CO_2 permeation, as shown in Fig. 9. The permeance for both membranes was decreased at a very low water activity, and then kept constant as the water activity increased. The silicon rubber membranes showed a constant permeance across all the range of water activity, but the permeance was approximately 100 times lower than that for the BTESE/Me-SiO_2-P and BTESO/Me-SiO_2-P membranes due to the increase in thickness (1000 μm).[15]

Fig. 10 illustrates the dimensionless permeance of CO_2 (DP) that is normalized by dry CO_2 permeance as a function of water activity compared with the other organosilica membranes. The DP values for BTESE and BTESO membranes coated on plasma-treated Me-SiO_2 intermediate layers (BTESE/Me-SiO_2-P, BTESO/Me-SiO_2-P) were 0.23 and 0.46 at water activity around 0.75, respectively. The two membranes showed much lower decrease in permeance than BTESE and BTESO membranes prepared on ZrO_2-SiO_2 intermediate layers with DP value of 0.01 and 0.08, respectively. Compared with the BTESE/Me-SiO_2 and BTESO/Me-SiO_2 membranes without plasma treatment, the BTESE/Me-SiO_2-P and BTESO/Me-SiO_2-P membranes showed a slightly larger decrease in permeance. This was because the hydrophilic groups such as the -OH groups, which were generated by the plasma treatment on Me-SiO_2 sub-layers, may not have been totally condensed with the Si-OH groups on the surface of the top layers (BTESE or BTESO). This could have resulted in higher water adsorption at the interface of the two layers. Since the membranes with plasma treatment showed high selectivity and lower decrease in permeance, it can be concluded that plasma treatment is an effective way to improve performance for both membranes.

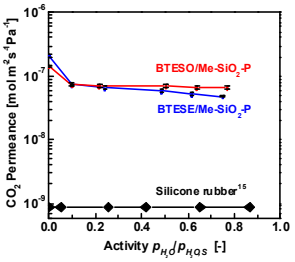

Fig. 9 CO_2 permeance of BTESE/Me-SiO_2-P and BTESO/Me-SiO_2-P membranes as a function of water activity at 40 °C.

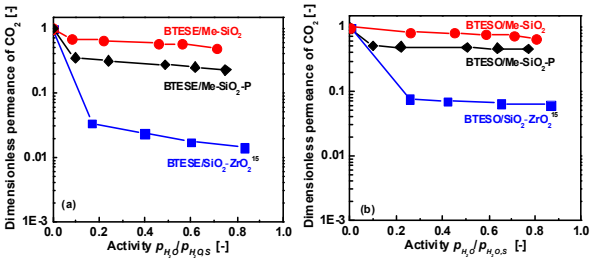

Fig. 10 Comparison of dimensionless permeance of CO_2 for (a) BTESE and (b) BTESO membranes coated on SiO_2-ZrO_2 and Me-SiO_2 with and without plasma in the presence of water vapor at 40 °C.

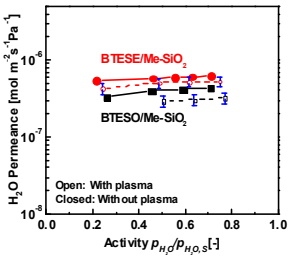

Fig. 11 Comparison of H_2O permeance for organosilica membrane as a function of water vapor activity at 40 °C (Conditions: Feed side: 500 ml/min, permeate side: 1000 ml/min)

Fig. 11 shows H_2O permeance as a function of water activity in the feed stream for BTESE/Me-SiO_2 and BTESO/Me-SiO_2 membranes with and without plasma treatment. Water permeance for the four organosilica membranes was much larger than CO_2 permeance, and it was approximately independent of the water activity. This was because water molecules had a higher diffusion due to a small diameter and high adsorption even through hydrophobic membranes. In addition, the hydrophobic organosilica membranes showed a long stability for CO_2 permeation in the presence of water vapor and liquid water (see Supporting information).

4. Conclusions

Organosilica membranes were prepared to form hydrophobic

top layers on hydrophobic intermediate layers via plasma-assisted multi-layered coatings. Multi-layered coating was confirmed to form hydrophobic Me-SiO_2 layers. H_2O plasma was optimized to generate hydrophilic groups on the hydrophobic surface of Me-SiO_2 layers in a thin film without changing either the bulk properties or pore size. After plasma treatment, BTESE formed homogenous and continuous films on Me-SiO_2 layers. Moreover, the plasma method improved the adhesion of BTESO films coated on Me-SiO_2 layers.

Under dry gas separation, the gas selectivity for BTESE membranes coated on plasma-treated Me-SiO_2 was improved. On the other hand, BTESO membranes showed no change after plasma treatment. In the presence of water vapor, CO_2 permeance showed a slightly larger decrease with plasma treatment than without it for both BTESE and BTESO membranes, but the decrease was much less than for the membranes with hydrophilic intermediate layers (SiO_2-ZrO_2).

References

1 L. N. Ho, J. P. Pellitero, F. Porcheron and R. J. M. Pellenq, *Langmuir,* 2011, **27,** 8187.
2 G. Li, T. Niimi, M. Kanezashi, T. Yoshioka and T. Tsuru, *Int. J. Hydrogen. Energ.,* 2013, **38,** 15302.
3 P. D. Chapman, T. Oliveira, A. G. Livingston and K. Li, *J. Membr. Sci.,* 2008, **318**, 5.
4 M. Elma, C. Yacou, D. K. Wang, S. Smart and J. C. D. Costa, *Water,* 2012, **4,** 629.
5 M. Pera-Titus, *Chem. Rev.,* 2014, **114,** 1413.
6 J. C. Poshusta, R. D. Noble and J. L. Falconer, *J. Membr. Sci.,* 2008, **186,** 25.
7 G. Xomeritakis, C. Y. Tsai and C. J. Brinker, *Sep. Purif. Technol.,* 2005, **42,** 249.
8 C. A. Scholes, S. E. Kentish and G. W. Stevens, *Sep. Purif. Rev.,* 2009, **38,** 1.
9 B. T. Low, L. Zhao, T. C. Merkel, M. Weber and D. Stolten, *J. membr. Sci.,* 2013, **431,** 139.
10 Q. Wei, F. Wang, Z. R. Nie, C. L. Song, Y. L. Wang and Q. Y. Li, *J. Phys. hem. B,* 2008, **112,** 9354.
11 N. A. Ahmad, C. P. Leo, A. L. Ahmad and W. K.W. Ramli, *Sep. Purif. Rev.,* 2015, **44,** 109.
12 S. Cerneaux, I. Struzyńska, W. M. Kujawski, M. Persin and A. Larbot, *J. Membr. Sci.,* 2009, **337,** 55.
13 C. C. Wei and K. Li, *Ind. Eng. Chem. Res.,* 2009, **48,** 3446.
14 R. M. de Vos, W. F. Maier and H.Verweij, *J. Membr. Sci.,* 1999, **158,** 277.
15 X. Ren, K. Nishimoto, M. Kanezashi, H. Nagasawa, T. Yoshioka and T. Tsuru, *Ind. Eng. Chem. Res.,* 2014, **5,** 6113.
16 J. H. Prosser, T. Brugarolas, S. Lee, A. J. Nolte and D. Lee, *Nano. Lett.,* 2012, **12,** 5287.
17 C. Depagne, S. Masse, T. Link and T. Coradin, J. *Mater. Chem.,* 2012, **22,** 12457.
18 M. Kanezashi, K. Yada, T. Yoshioka and T. Tsuru, *J. Am. Chem. Soc.,* 2009, **131,** 414.
19 M. C. Duke, J. C. D. Costa, D. D. Do, P. G. Gray and G.Q. Lu, *Adv. Funct. Mater.,* 2006, **16,** 1215.
20 S. M. Ibrahim, R. Xu, H. Nagasawa, A. Naka, J. Ohshita, T. Yoshioka, M. Kanezashi and T. Tsuru, *RSC Adv.,* 2014, **4,** 23759.
21 R. Xu, J. H. Wang, M. Kanezashi, T. Yoshioka and T. Tsuru, *ACS Appl. Mater. Interfaces,* 2013, **5,** 6147.
22 L. L. Pranevicius, D. Milcius, S. Tuckute and K. Gedvilas, *Appl. Sur. Sci.,* 2012, **258,** 8619.
23 A. Pakdel, Y. Bando and D. Golberg, *Nano.,* 2014, **8,** 10631.
24 J. Choi, S. Choi, Y. Kang, S. Na, H-J. Lee, M-H. Cho and H. Kim, *ACS Appl. Mater. Interfaces,* 2014, **6,** 14712.
25 K. Zarshenas, A. Raisi and A. Aroujalian, *RSC Adv.,* 2015, **5,** 19760.
26 Y. Ma, M. Kanezashi and T. Tsuru, *J. Sol-Gel. Sci. Technol.,* 2010, **53,** 93.
27 T. Tsuru, T. Nakasuji, M. Oka, M. Kanezashi and T. Yoshiok, *J. Membr. Sci.,* 2011, **384,** 149.
28 Z. Olejniczak, M. Łeczka, K. C-Kowalska, K. Wojtach, M. Rokita and W. Mozgawa, *J. Mol. Struct.,* 2005, **744-747,** 465.
29 H. H. El-Feky, K. B. Briceño, E. O. Jardim, J. S. Albero and T. Gumí, *Microporous and Mesoporous Mater.,* 2013, **179,** 22.
30 L. Meagher and R. M. Pashley, J. Coll. Int. Sci. 1997, **185,** 291.
31 T. Nakagawa and M. Soga, *Jpn. J. Appl. Phys.,* 1997, **36,** 6915.
32 M. L. Steen, L. Hymas, E. D. Havey, N. E. Capps, D. G. Castner and E. R. Fisher, *J. Membr. Sci.,* 2001, **188,** 97.
33 T. Tsuru, T. Hino, T. Yoshioka and M. Asaeda, *J. Membr. Sci.,* 2001, **186,** 257.